Enhanced Detectivity and Suppressed Dark Current of Perovskite–InGaZnO Phototransistor via a PCBM Interlayer

Xiaote Xu,[†] Lizhi Yan,[†] Taoyu Zou,[†] Renzheng Qiu,[†] Chuan Liu,[‡] Qing Dai,[§] Jun Chen,[‡] Shengdong Zhang,[†] and Hang Zhou*[,†]

[†]School of Electronic and Computer Engineering, Peking University Shenzhen Graduate School, Shenzhen 518055, China

[‡]State Key Laboratory of Optoelectronic Materials and Technologies, School of Electronics and Information Technology, Sun Yat-Sen University, Guangzhou 510006, China

[§]National Center for Nanoscience & Technology, Chinese Academy of Sciences, Beijing 100190, China

Supporting Information

ABSTRACT: Hybrid phototransistors based on InGaZnO (IGZO) metal oxide thin-film transistors (TFT) and a photoabsorbing capping layer such as perovskite ($MAPbI_3$) are a promising low-cost device for developing advanced X-ray and UV flat-panel imagers. However, it is found that the introduction of $MAPbI_3$ inevitably damages the IGZO channel layer during fabrication, leading to deteriorated TFT characteristics such as off-current rising and threshold voltage shift. Here, we report an effective approach for improving the performance of the perovskite–IGZO phototransistor by inserting a [6,6]-phenyl C61-butyric acid methyl ester (PCBM) or PCBM:PMMA interlayer between the patterned $MAPbI_3$ and IGZO. The interlayer effectively prevents the IGZO from damage by the perovskite fabrication process, while allowing efficient charge transfer for photosensing. In this configuration, we have achieved a high-detectivity (1.35×10^{12} Jones) perovskite–IGZO phototransistor with suppressed off-state drain current (~10 pA) in the dark. This work points out the importance of interface engineering for realizing higher performance and reliable heterogeneous phototransistors.

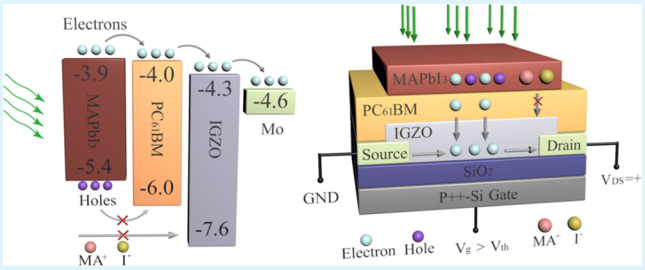

KEYWORDS: *IGZO, perovskite, interlayer, photodetector, phototransistor*

1. INTRODUCTION

Integration of organic and inorganic materials provides new opportunities for realizing advanced optoelectronic devices that combine the unique advantages of each integrated component. Thin-film transistors (TFT) based on indium gallium zinc oxide (IGZO), which has the merits of a high field-effect carrier mobility and low off current,[1−3] are considered as a competitive backplane technology for display devices and imagers. However, when functioning as a phototransistor for photodetection or image-sensing applications, with an optical bandgap of about 3.5 eV,[3] IGZO is not sensitive to most visible or near-infrared light. Even for UV detection, the long decay time after light off, which is known as the persistent photoconductivity (PPC),[3] would still hinder its application in a circumstance where fast response or a high frame rate is needed. To extend its ability for photodetection, hybrid IGZO phototransistors were investigated with different types of light-absorber capping layers, such as polymer (P3HT and PCDTBT),[4,5] quantum dots (CdSe QDs, graphene dots, CdSe/ZnS QD, PbS QD),[6−9] and two-dimensional materials (MoS_2, WSe_2).[10,11]

Organolead halide perovskite, such as $MAPbI_3$, has been actively investigated in optoelectronic applications, due to its outstanding features such as a broad absorption range, tunable bandgap, high charge carrier mobility, and long carrier diffusion length.[12−15] One of the great advantages of this material is that it can be processed at a relatively low temperature (80–150 °C), which enables its integration with other functional materials on flexible substrates. Moreover, its compositional heavy elements such as lead and iodine ions render it a suitable material for high-energy radiation detection, such as X-ray.[16] Various types of photodetectors have been reported, such as phototransistors, photodiodes, and photoconductors.[17−19] Nonetheless, perovskite phototransistors show bipolar characteristics with the unstable off-state drain current at room temperature, and suffer from severe hysteresis due to strong ion migration.[20,21] To tackle these issues, some hybrid approaches have been proposed, with perovskite stacking on a transistor for example.[22,23] Capping the oxide-based TFT with an organolead halide perovskite photoabsorber is another attempt to combine the merits of these two materials.[2] The perovskite–IGZO hybrid phototransistor, in theory, should be able to provide a low off-state drain current and sensitive photoresponse to lights from the UV to visible

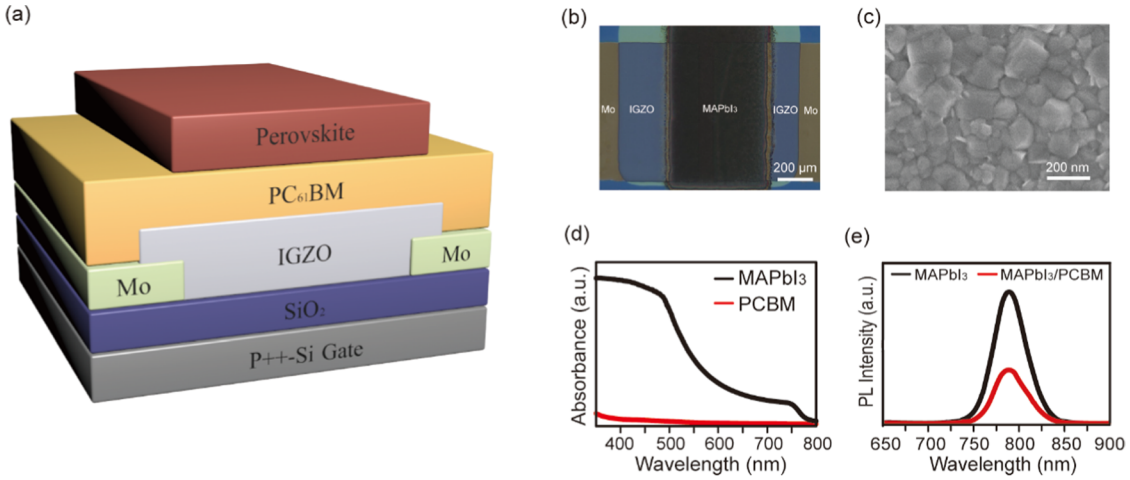

Figure 1. (a) Schematic diagram of the fabricating process of a perovskite–InGaZnO hybrid phototransistor; (b) top view of the perovskite–InGaZnO phototransistor under an optical microscope; (c) scanning electron microscope (SEM) image of the patterned perovskite layer; (d) optical absorbance of the fabricated $MAPbI_3$ and PCBM thin films on glass substrates; (e) photoluminescence spectra of the $MAPbI_3$ and $MAPbI_3$/PCBM thin films.

region, and even to infrared. However, there is evidence that the perovskite capping layer would raise the off-state dark current of oxide-based TFTs. In our previous work, a perovskite–IGZO heterojunction phototransistor for visible light detection was reported to have an off-state dark current that is 1 order of magnitude higher than that of the IGZO-only phototransistor.[2] Tak et al. also reported a similar off-state dark current rising issue in the IGZO/perovskite phototransistor, in which they reduced the thickness of the perovskite layer to minimize the dark current rising.[24] The rise of off-state dark current can be ascribed to the extra defects at the back channel of the oxide TFT created during perovskite deposition, or to the bypass channel created by direct contact of the perovskite layer with the source and drain electrode. Therefore, care must be taken to minimize these negative effects when bringing the perovskite on top of oxide TFTs.

Here, we introduce a [6,6]-phenyl C61-butyric acid methyl ester (PCBM) interlayer to protect the IGZO back channel, while maintaining efficient charge transfer between the IGZO and $MAPbI_3$. [6,6]-Phenyl C61-butyric acid methyl ester (PCBM) is a common electron-transporting layer that is frequently used in perovskite-based solar cells and photodetectors.[25,26] It has been shown that C60 and its derivatives may suffer from significant structural change on exposure to UV or X-ray at extreme intensity, due to the photoablation effect.[27−29] In our device configuration, PCBM is sandwiched between the perovskite and the IGZO layer. The perovskite with a high absorption coefficient for incoming light can protect the bottom PCBM and IGZO layers from irradiation damage. The phototransistor is also designed with patterned perovskite and a bottom source/drain contact structure to avoid leakage current. A new type of perovskite–IGZO phototransistor is successfully achieved with suppressed dark current and enhanced detectivity.

2. EXPERIMENTAL SECTION

2.1. Device Fabrication. To fabricate the coplanar structured IGZO TFT, 30 nm-thick molybdenum used as source/drain electrodes were deposited on a clean P++-doped Si wafer coated with 300 nm SiO_2 and followed by a photolithographic lift-off process. A 40 nm-thick IGZO film was deposited and then patterned by wet-etching to define the channel. At last, the devices were annealed in a furnace in O_2 atmosphere at 250 °C for 1 h. The channel length (L) and width (W) were 60 and 600 μm, respectively. To fabricate the PCBM interlayer, a 20 mg mL^{-1} solution of PCBM was synthesized by dissolving PCBM in dichlorobenzene and heating at 70 °C overnight. The PCBM solution was spin-coated on the substrate at 2000 rpm for 40 s and then annealed on a hot plate at 100 °C for 10 min. To fabricate the perovskite capping layer, 200 nm-thick patterned PbI_2 was thermal evaporated using a shadow mask and followed by spin-coating MAI solution at 3000 rpm for 40 s and then heated on a hot plate at 100 °C for 30 min. The 30 mg mL^{-1} solution of MAI was synthesized by dissolving MAI in isopropanol and heating at 70 °C overnight.

2.2. Characterization. The surface morphology of the perovskite films was observed using a scanning electron microscope (SEM, Carl Zeiss SUPRA 55 and VEGA3 TESCAN). The UV–visible absorption spectrum was measured by a UV–vis spectrophotometer (Shimadzu UV-2600). X-ray diffraction pattern data were collected with a Bruker D8 Advance diffractometer with nickel-filtered Cu Kα radiation (1.5406 Å) operating at 40 kV and 40 mA. Photoluminescence (PL) spectra were obtained using a 1 K series He–Cd laser. Electrical characteristics and photoresponse of the phototransistors were tested using an Agilent B1500 semiconductor parameter analyzer under dark and illuminated conditions. Lights of various wavelengths were provided by a 500 W Xenon arc lamp and Monochromators (Zolix Omni-λ). The incident optical power was measured by a high-sensitivity power meter (Newport 818-UV-DB).

3. RESULTS AND DISCUSSION

Figure 1a illustrates the device structure of the perovskite–IGZO hybrid phototransistor with a PCBM interlayer. A schematic of the fabrication process can be found in Figure S1. To fabricate the device, first, a bottom gate bottom contact IGZO TFT was fabricated with 60 μm channel length (L) and 600 μm width (W). Then, a PCBM interlayer (~30 nm) was deposited by spin-coating. Next, a patterned PbI_2 layer with an area of 600 μm × 1000 μm was thermal evaporated on top of the IGZO channel region, followed by spin-coating the MAI precursor, and annealing at 100 °C to form a patterned $MAPbI_3$ perovskite photoabsorbing layer. The optical microscopy image of the device is shown in Figure 1b. In such a configuration, the patterned perovskite acts as the light absorber without contacting the source/drain electrode, which is supposed to guarantee a low off-state dark current for the IGZO TFT. The surface morphology of the resultant

compact $MAPbI_3$ layer is shown in Figure 1c, which comprises of large crystal grains in the range of hundreds of nanometers. UV−vis absorption spectra of $MAPbI_3$ and PCBM are shown in Figure 1d. The $MAPbI_3$ top layer with an absorption coefficient much higher than that of PCBM would, therefore, absorb most of the incident photons from the ultraviolet to visible region (from 350 to 780 nm). Figure 1e compares the PL intensity of a perovskite-only thin film and a perovskite/PCBM thin film. It can be observed that the PL intensity of the perovskite layer is significantly quenched when a PCBM layer is inserted, which shows that photogenerated charge (electrons) can be effectively transferred from $MAPbI_3$ to PCBM. A similar charge-transfer process was reported from the PCBM layer to the IGZO layer in previous investigations.[1]

To verify the importance of the perovskite-patterning steps and of the PCBM interlayer, hybrid IGZO phototransistors without a PCBM interlayer were fabricated by spinning the perovskite layers onto the IGZO TFT. As shown in Figure 2,

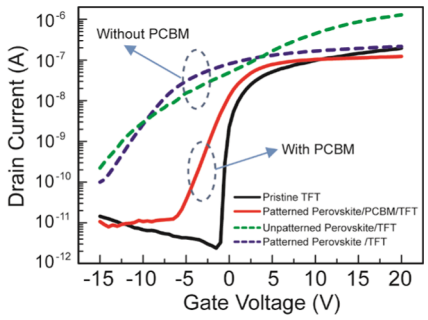

Figure 2. Transfer characteristics (V_d = 2 V) of pristine TFT, the patterned perovskite/PCBM/TFT device, the unpatterned perovskite/TFT device, and the patterned perovskite/TFT device.

capping the perovskite by the spin-coating process severely deteriorates the performance of a phototransistor. By the spin-coating process, the contact between the perovskite and the source/drain is unavoidable, which could be one of the possible reasons for the large leakage current. Nonetheless, the patterned perovskite without the PCBM interlayer still causes a significant rise in the off-state drain current, which could probably be due to the extra defects at the back channel of the IGZO TFT created during perovskite deposition. To identify which perovskite fabrication step and composition (MA^+ or I^-)[30,31] is responsible for the deterioration of the IGZO TFT, further investigations were carried out by depositing both patterned and unpatterned PbI_2 or MAI layer at the back of the IGZO channel. In Figure S3a, it can be found that both unpatterned spin-coated PbI_2 film and MAI film can cause serious deviation of the transfer characteristics from the pristine IGZO TFT, whereas with the patterning process, as shown in Figure S3b,c, the patterned MAI layer brings significantly higher damage on the IGZO TFT than the patterned PbI_2 layer. From these results, it can be concluded that MA^+ is the main reason for causing the malfunction of the IGZO TFT. To counter this problem, an interlayer is required for effective charge transportation and restriction of MA^+ ion migration from the perovskite layer. Figure S3d shows that by inserting a PCBM interlayer and patterning the MAI, a good transfer characteristic (I_d−V_g) with a fair on/off current ratio and low off-state current can be achieved from the IGZO phototransistor.

The details of the TFT device parameters with and without a perovskite/PCBM capping layer is shown in Table 1, where V_{th} denotes the threshold voltage and S.S stands for the subthreshold swing of the TFT (for the extraction method, refer to Figure S2). The off-state dark current of the hybrid phototransistor reaches 2.36×10^{-11} A when biased as −5 V, leading to an on/off current ratio I_{on}/I_{off} of 10^4, which is comparable to that of pristine IGZO TFT without perovskite/PCBM capping layers, and is much smaller than those of most of the reported IGZO-based phototransistors (see Table S1).

To evaluate the photodetection performance of the perovskite−IGZO phototransistor, the transfer characteristics (I_d−V_g) of the perovskite−IGZO phototransistors under the illumination of different wavelengths of monochromatic light and under different illumination intensities are presented in Figure 3a,b, respectively. The device shows a wide response from the ultraviolet to visible region in Figure 3a, with an obvious decrease in the photocurrent at ∼800 nm, which is close to the bandgap of the perovskite capping layer. Besides, the device even shows a remarkable photocurrent in the on-state region, where the gate bias voltage is bigger than the threshold voltage ($V_g > V_{th}$), when illuminated with a wavelength shorter than 700 nm. It is noted that the change of current with wavelength (350−700 nm) at V_g = −5 V is different from that at V_g = 15 V. For example, when illuminated at 350 nm, the photocurrent of perovskite/IGZO TFT is the lowest at V_g = −5 V and becomes the highest at V_g = 15 V as shown in Figure 3a. It is suspected that this phenomenon is related to the optical absorption length and the carrier drift/diffusion mechanism in the perovskite layer. When the perovskite layer is illuminated under short-wavelength light, most of the photogenerated electron hole pairs are created at the top surface of the perovskite layer. Under negative gate bias, the photogenerated electrons have to diffuse a long distance across the whole perovskite layer to reach the PCBM interlayer, which leads to heavy recombination loss during diffusion. In contrast, when operated at V_g = 15 V, the applied positive bias could attract the electrons to drift to the bottom interface, which effectively reduces the photogenerated carrier recombination loss, resulting in a higher current under short-wavelength light illumination. For longer wavelengths, due to the long optical absorption length, the photogenerated carriers are created in the whole perovskite layer. In this case, the average carrier diffusion distance is within the diffusion length, and the effect of gate bias on the on-state photocurrent is then not as significant as that in the case of short-wavelength illumination. Figure 3b shows the transfer characteristics of the perovskite−IGZO phototransistor when illuminated under 550 nm with the light intensity varying from 0.008 to 0.754 mW cm^{-2}. It can be found that the hybrid phototransistor responds

Table 1. IGZO TFT and Perovskite−IGZO Phototransistor Parameters

structures	V_{th} (V)	S.S (V dec^{-1})	I_{off} (A)	I_{on} (A)
IGZO	−1.04 ± 1.13	0.25 ± 0.06	(6.71 ± 2.0) × 10^{-12}	(1.96 ± 0.1) × 10^{-7}
$MAPbI_3$/PCBM/IGZO	−0.33 ± 0.98	1.92 ± 0.05	(2.36 ± 1.1) × 10^{-11}	(2.95 ± 0.1) × 10^{-7}

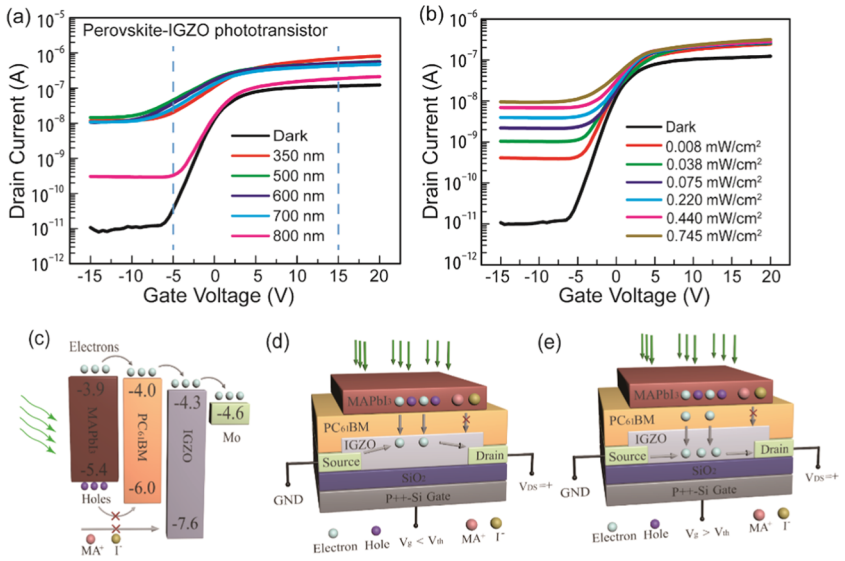

Figure 3. Transfer characteristics of (a) perovskite−IGZO phototransistors under various wavelengths of incident light and (b) different incident light intensities at 550 nm (V_d = 2 V). (c) Schematic of the energy-band diagram of $MAPbI_3$, PCBM, IGZO, and the photogenerated charge transportation (data are adapted from refs 1 and 2). (d) Schematics of the photodetection mechanism of perovskite−IGZO hybrid phototransistors under negative gate bias ($V_g < V_{th}$) and (e) positive gate bias ($V_g > V_{th}$).

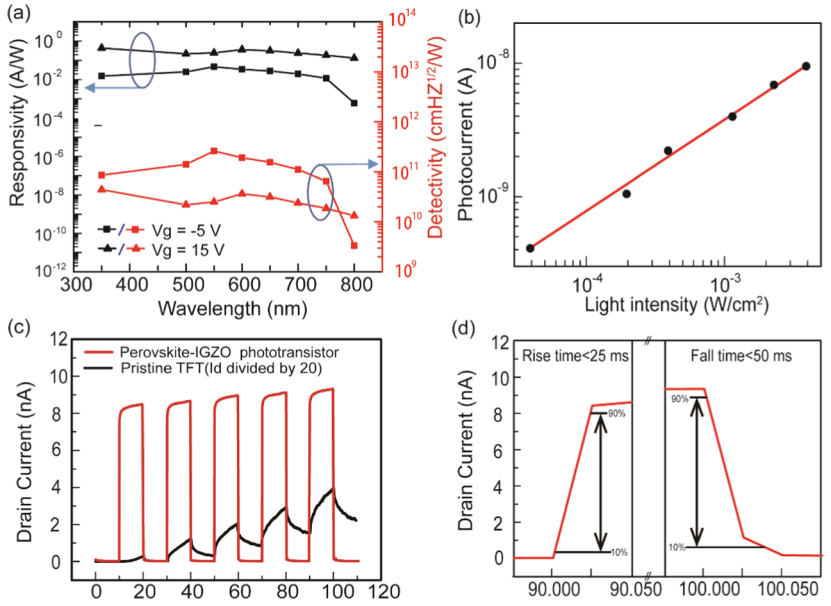

Figure 4. (a) Photoresponsivity and detectivity of perovskite−IGZO phototransistor at V_d = 2 V, V_g = −5 V and V_d = 2 V, V_g = 15 V; (b) linear dynamic range of the device; (c) transient response of IGZO TFTs and perovskite−IGZO phototransistors under 350 nm pulse light at V_d = 2 V, V_g = −10 V; (d) transient response of perovskite−IGZO phototransistors to 350 nm light with a rise time less than 25 ms and fall time less than 50 ms.

well to the weak light signal due to its low off-state dark current, and the photoinduced drain current increased linearly with the incident light intensity when the TFT operates at the off-state ($V_g < V_{th}$).

A device working mechanism of the perovskite−IGZO hybrid phototransistors is proposed and sketched in Figure 3c−e. When operated at $V_g < V_{th}$, the transistor is working in the turn-off regime. The free carrier-depleted IGZO channel leads to the low drain current in the dark. When illuminated, excitons would be generated in the perovskite photoabsorbing layer. Meanwhile, due to the low exciton-binding energy, excitons can be easily separated into free carriers in the perovskite thin film or at the perovskite/PCBM interface.[32] However, the deep LUMO level of the PCBM layer and the valence band of IGZO would block the photogenerated holes, as sketched in Figure 3c. The band alignment only allows the transportation of photogenerated electrons from the perovskite to the back channel of IGZO via the PCBM interlayer, whereas holes are blocked and accumulated in the perovskite layer. Vertically, the device is similar to the open-circuit condition of a solar cell without the hole transport layer; the holes remain in the perovskite and the electrons are accumulated at the bottom of the PCBM and are responsible for the current at the back channel of IGZO TFT.[33,34] As the gate is negative biased, the electron will be repelled from the IGZO/SiO_2 interface; it is suspected that the transferred electron would only travel at the

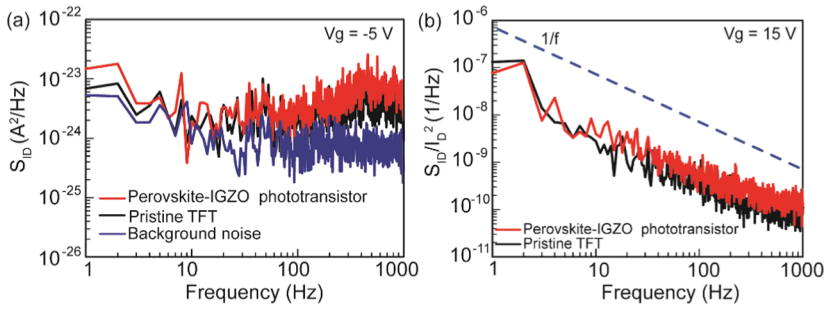

Figure 5. (a) Drain current noise spectral density (S_{ID}) at V_d = 2 V, V_g = −5 V. (b) Normalized drain current noise spectral density (S_{ID}/I_D^2) at V_d = 2 V, V_g = 15 V.

back channel of the IGZO TFT. When operated at on-state ($V_g > V_{th}$), electrons start to accumulate at the IGZO/SiO_2 interface in the dark, creating a conductive path known as a front channel. Upon illumination, the photogenerated electrons from the perovskite layer would add to the electron concentration at the accumulation region, leading to an increase in the on-state current.

The key parameters to quantify a phototransistor are responsivity (R) and detectivity (D^*), which can be calculated by the following equations

$$R = \frac{I_{\text{d-ph}} - I_{\text{d-dark}}}{P_{\text{in}}} \tag{1}$$

$$D^* = \frac{R}{(2qI_{\text{d-dark}}/A)^{1/2}} \tag{2}$$

where $I_{\text{d-ph}}$ and $I_{\text{d-dark}}$ are the drain current under illumination and dark condition, respectively, P_{in} is the power of the incident light, q is the elementary charge (1.6×10^{-19} C), and A is the effective area of the detector. Equation 2 is valid when the shot noise is assumed to be mainly from the dark current.[35] As shown in Figure 4a, the perovskite−IGZO hybrid phototransistor shows a decent and stable responsivity larger than 10 mA W^{-1}, when V_g is biased at −5 V for wavelengths between 350 and 750 nm, reaching a maximum value of 244.3 mA W^{-1} at 550 nm under a power density of 0.754 mW cm^{-2}. The responsivity is about 1 order of magnitude larger when V_g is biased at V_g = 15 V due to a larger photocurrent. Compared with the IGZO phototransistor, due to the photoabsorption of the perovskite layer, the perovskite/IGZO phototransistor shows light-detecting ability to near-infrared light (800 nm). The responsivity of the perovskite−IGZO hybrid phototransistor is comparable to some reported IGZO-based hybrid phototransistors like MoS_2/IGZO or other perovskite photodetectors.[11,19]

The detectivity of the perovskite−IGZO hybrid phototransistor reaches 1.35×10^{12} Jones at 550 nm under the power intensity of 0.754 mW cm^{-2}, which is more than 2 orders of magnitude higher than the previously reported $MAPbI_3$/IGZO hybrid phototransistor ($D^* = 9.5 \times 10^8$ J) due to the lower dark current in off-state.[2]

The linearity of the photoresponse to the light intensity of a photodetector is often characterized by linear dynamic range (LDR), which can be expressed as

$$\text{LDR} = 20 \log \frac{I_{\text{ph-max}}}{I_{\text{dark}}} \tag{3}$$

Here, $I_{\text{ph-max}}$ is the maximum photocurrent within the linear region. The calculated LDR at 550 nm is 59 dB, as shown in Figure 4b. The calculated LDR is much larger than that of our previously reported nonpatterned hybrid device (31 dB) due to the reduced dark current.[2] The LDR of the perovskite−IGZO phototransistor is currently limited by the maximum power intensity of our light source. As most of the photocurrent at the TFT on-state region is saturated at around 10^{-7} A, the theoretical maximum linear photocurrent is estimated to be in the same order, which gives a theoretical LDR of around 80 dB.

The transient responses of the perovskite−IGZO phototransistor were measured by periodic illumination with an on/off interval of 10 s. The perovskite−IGZO hybrid phototransistor was measured at V_d = 2 V and V_g = −10 V under illumination with a light intensity of 0.707 mW cm^{-2} at 350 nm. The rise time or fall time is defined as the time interval between 10 and 90% of the peak value of the photocurrent when the light is on or off. As shown in Figure 4c, for the IGZO TFT, the drain current decays slowly after the light is turned off (more than 10 s) and it increases rapidly after several periods of illumination. This is known as the persistent photoconductivity (PPC) phenomenon, which is caused by the ionization of oxygen vacancy sites under the light, especially in the ultraviolet region.[3] The transient response of the perovskite−IGZO hybrid phototransistors to 350 nm light in one period is shown in Figure 4d. After capping the perovskite light absorber, the phototransistor features a fast transient response with an abrupt rise and fall time within tens of milliseconds and the characteristic remains unchanged for a long measurement time. To further exclude the effect of the photoresponse of IGZO, the transfer characteristics of IGZO transistors under visible light with the wavelength ranging from 450 to 700 nm were measured and are shown in Figure S4a; the photoresponse effect of the IGZO phototransistor at V_g = −5 V to light longer than 500 nm becomes negligible. We further tested the transient response of the perovskite/IGZO device under 550 nm light with V_g = −5 V and V_{ds} = 2 V, which is shown in Figure S4b. The perovskite/IGZO phototransistor exhibits a similar fast transient response features with an abrupt rise and fall time of less than 40 and 28 ms.

Details of the performance parameters of some reported photodetectors are listed in Table S1. The fast transient response comes from the effective transportation of electron form $MAPbI_3$ to IGZO via the PCBM interlayer. Besides, the PPC phenomenon of the IGZO under illumination is prevented, as most of the incident light is absorbed by the $MAPbI_3$ light absorber.

The noise current level of the photodetector is another key parameter that deserves to be investigated, especially when designing a readout circuit for the photodetectors that would amplify the noise signal as well. Here, the low-frequency noise (LFN) characteristics of the pristine TFT and the perovskite−IGZO phototransistor under positive and negative gate bias are compared in the frequency range of 1 Hz to 1 kHz. In Figure 5a, both the pristine IGZO TFT and the perovskite−IGZO TFT show a noise level close to the equipment's background white noise when V_g = −5 V. This is probably due to the extremely low dark current level obtained from the TFTs. In contrast, the normalized drain-current noise spectral densities, S_{ID}/I_D, fit well to the $1/f$ relationship as shown in Figure 5b, which indicates that the low-frequency noise of drain current of IGZO TFT and perovskite−IGZO TFT obeys the classical $1/f$ noise theory. The obtained data agree well with the previous study on the LFN characteristics of IGZO TFTs.[36,37] The above results indicate that the integration of $MAPbI_3$ light absorption layer does not affect the LFN characteristic of the underlying IGZO TFTs.

To further reduce the off-state drain current and increase the stability, we also investigated the effect of the blended PCBM:PMMA interlayer (poly(methyl methacrylate) (PMMA) wt = 25%). Compared with the PCBM thin film, the PMMA polymer can form a relatively more compact gel-like thin film during the spin-coating process. An interlayer with a mixture of the appropriate proportion of PCBM and PMMA could form a compact conductive composite polymer that protects the IGZO transistor from potential ion-diffusion damages during the perovskite fabrication process. Thus, the perovskite/IGZO TFT with a PMMA/PCBM layer can maintain a dark off-state current level similar to that of the original IGZO TFT. Besides, since IGZO is sensitive to moisture, PMMA can help encapsulate the bottom IGZO TFT. The transfer characteristic of the PCBM:PMMA interlayered device is shown in Figure 6: the off-state drain current of the PCBM:PMMA device is almost the same as that of pristine IGZO TFT. The result shows that the PCBM:PMMA interlayer can further restrain ion diffusion from perovskite to IGZO and thus leads to a lower off-state drain current. However, the mixture of PMMA decreases the electric conductivity of the interlayer, which leads to the reduced photocurrent. The blended PCBM:PMMA interlayer provides a way to further optimize the device by adjusting the proportion of PMMA to compromise the dark off-state drain current and photocurrent to get better responsivity and detectivity.

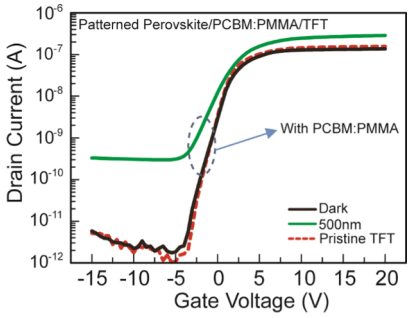

Figure 6. Transfer characteristics (V_d = 2 V) of a patterned perovskite/PCBM:PMMA/IGZO TFT device under dark and light illumination.

4. CONCLUSIONS

In conclusion, we demonstrated a high-performance perovskite−IGZO hybrid phototransistor with suppressed dark current, broad-spectrum response, and a fast transient response time. The device exhibits a sensitive response from ultraviolet to visible light and extends its sensing ability to the near-infrared region when operating in the off-state region. It also obviates the persistent photoconductivity behavior of metal oxide phototransistors in the ultraviolet region with a fast transient response within tens of milliseconds. The dark current of the device remains at a remarkably low value of 10 pA, which is smaller than that of most of the reported photodetectors. The performance parameters of the perovskite−IGZO hybrid phototransistor is comparable to or even better than the reported perovskite photodetectors or IGZO-based phototransistors. This work provides a new way to integrate a light absorber with a metal oxide semiconductor in the photodetection area, which has great potential applications in low-cost and flexible image sensors.

■ ASSOCIATED CONTENT

Supporting Information

$I_D^{1/2}$−V_g characteristics (Figure S1); schematics of the different device structure (Figure S2); transfer characteristics of TFT capped with PbI_2 or MAI (Figure S3); transfer characteristics of IGZO transistors under various wavelengths of incident light and transient response of perovskite−IGZO phototransistors to 550 nm light (Figure S4); transfer characteristics of phototransistors after 30 days (Figure S5); comparison of the performance parameters IGZO- and perovskite-based photodetector (Table S1) (PDF)

■ AUTHOR INFORMATION

Corresponding Author

*E-mail: zhouh81@pkusz.edu.cn.

ORCID

Jun Chen: 0000-0001-7397-2714

Hang Zhou: 0000-0002-0472-9515

Author Contributions

H.Z. conceived the idea and supervised the project; X.X. performed the experiments and carried out the measurements; X.X., L.Y., and T.Z. collected and analyzed the data; R.Q. provided assistance in the experimental set up; C.L. and S.Z. gave important discussions for the performance of the experiments; Q.D. and J.C. participated in the data analysis and interpretation. All of the authors discussed the results and revised the manuscript.

Notes

The authors declare no competing financial interest.

■ ACKNOWLEDGMENTS

This work is financially supported by the National Key Research and Development Program of China (2016YFA0202002), Guangdong Natural Science Foundation (2018A030313332), and the Shenzhen Science and Technology Innovation Foundation (JCYJ20160229122349365). C.L. would like to acknowledge the Science and Technology Program of Guangdong Province (Grant No.

2015B090924001), Guangdong Natural Science Funds for Distinguished Young Scholars (Grant No. 2016A030306046).

REFERENCES

(1) Rim, Y. S.; et al. Ultrahigh and broad spectral photodetectivity of an organic−inorganic hybrid phototransistor for flexible electronics. *Adv. Mater.* **2015**, *27*, 6885−6891.

(2) Du, S.; Li, G.; Cao, X.; Wang, Y.; Lu, H.; Zhang, S.; Liu, C.; Zhou, H. Oxide Semiconductor Phototransistor with Organolead Trihalide Perovskite Light Absorber. *Adv. Electron. Mater.* **2017**, *3*, No. 1600325.

(3) Jeon, S.; Ahn, S. E.; Song, I.; Kim, C. J.; Chung, U. I.; Lee, E.; Yoo, I.; Nathan, A.; Lee, S.; Robertson, J.; Kim, K. Gated three-terminal device architecture to eliminate persistent photoconductivity in oxide semiconductor photosensor arrays. *Nat. Mater.* **2012**, *11*, 301−305.

(4) Zan, H.-W.; Hsueh, H.-W.; Kao, S.-C.; Chen, W.-T.; Ku, M.-C.; Tsai, W.-W.; Tsai, C.-C.; Meng, H.-F. P-25: New Polymer-Capped a-IGZO TFT with High Sensitivity to Visible Light for the Development of Integrated Touch Sensor Array. *SID Symp. Dig. Tech. Pap.* **2010**, *41*, 1316−1318.

(5) Wang, H.; Xiao, Y.; Chen, Z.; Xu, W.; Long, M.; Xu, J.-B. Solution-processed PCDTBT capped low-voltage InGaZnOx thin film phototransistors for visible-light detection. *Appl. Phys. Lett.* **2015**, *106*, No. 242102.

(6) Shin, S. W.; Lee, K. H.; Park, J. S.; Kang, S. J. Highly Transparent, Visible-Light Photodetector Based on Oxide Semiconductors and Quantum Dots. *ACS Appl. Mater. Interfaces* **2015**, *7*, 19666−19671.

(7) Pei, Z.; Lai, H.-C.; Wang, J.-Y.; Chiang, W.-H.; Chen, C.-H. High-Responsivity and High-Sensitivity Graphene Dots/a-IGZO Thin-Film Phototransistor. *IEEE Electron Device Lett.* **2015**, *36*, 44−46.

(8) Cho, J. E.; Yu, J.; Kang, S. J. Visible light−modulated phototransistors based on ZnO and CdSe/ZnS quantum dots. *Curr. Appl. Phys.* **2016**, *16*, 1560−1563.

(9) Hwang, D. K.; Lee, Y. T.; Lee, H. S.; Lee, Y. J.; Shokouh, S. H.; Kyhm, J.-h.; Lee, J.; Kim, H. H.; Yoo, T.-H.; Nam, S. H.; Son, D. I.; Ju, B.-K.; Park, M.-C.; Song, J. D.; Choi, W. K.; Im, S. Ultrasensitive PbS quantum-dot-sensitized InGaZnO hybrid photoinverter for near-infrared detection and imaging with high photogain. *NPG Asia Mater.* **2016**, *8*, No. e233.

(10) Guo, N.; Gong, F.; Liu, J.; Jia, Y.; Zhao, S.; Liao, L.; Su, M.; Fan, Z.; Chen, X.; Lu, W.; Xiao, L.; Hu, W. Hybrid WSe2-In2O3 Phototransistor with Ultrahigh Detectivity by Efficient Suppression of Dark Currents. *ACS Appl. Mater. Interfaces* **2017**, *9*, 34489−34496.

(11) Yang, J.; Kwak, H.; Lee, Y.; Kang, Y. S.; Cho, M. H.; Cho, J. H.; Kim, Y. H.; Jeong, S. J.; Park, S.; Lee, H. J.; Kim, H. MoS2-InGaZnO Heterojunction Phototransistors with Broad Spectral Responsivity. *ACS Appl. Mater. Interfaces* **2016**, *8*, 8576−8582.

(12) Xu, X.; Li, S.; Zhang, H.; Shen, Y.; Zakeeruddin, S. M.; Graetzel, M.; Cheng, Y. B.; Wang, M. A power pack based on organometallic perovskite solar cell and supercapacitor. *ACS Nano* **2015**, *9*, 1782−1787.

(13) Li, G.; Tan, Z. K.; Di, D.; Lai, M. L.; Jiang, L.; Lim, J. H.; Friend, R. H.; Greenham, N. C. Efficient light-emitting diodes based on nanocrystalline perovskite in a dielectric polymer matrix. *Nano Lett.* **2015**, *15*, 2640−2644.

(14) Jaramillo-Quintero, O. A.; Sanchez, R. S.; Rincon, M.; Mora-Sero, I. Bright Visible-Infrared Light Emitting Diodes Based on Hybrid Halide Perovskite with Spiro-OMeTAD as a Hole-Injecting Layer. *J. Phys. Chem. Lett.* **2015**, *6*, 1883−1890.

(15) Li, W.; Dong, H.; Dong, G.; Wang, L. Hystersis mechanism in perovskite photovoltaic devices and its potential application for multi-bit memory devices. *Org. Electron.* **2015**, *26*, 208−212.

(16) Yakunin, S.; Sytnyk, M.; Kriegner, D.; Shrestha, S.; Richter, M.; Matt, G. J.; Azimi, H.; Brabec, C. J.; Stangl, J.; Kovalenko, M. V.; Heiss, W. Detection of X-ray photons by solution-processed organic-inorganic perovskites. *Nat. Photonics* **2015**, *9*, 444−449.

(17) Li, F.; Ma, C.; Wang, H.; Hu, W.; Yu, W.; Sheikh, A. D.; Wu, T. Ambipolar solution-processed hybrid perovskite phototransistors. *Nat. Commun.* **2015**, *6*, No. 8238.

(18) Bao, C.; Zhu, W.; Yang, J.; Li, F.; Gu, S.; Wang, Y.; Yu, T.; Zhu, J.; Zhou, Y.; Zou, Z. Highly Flexible Self-Powered Organolead Trihalide Perovskite Photodetectors with Gold Nanowire Networks as Transparent Electrodes. *ACS Appl. Mater. Interfaces* **2016**, *8*, 23868−23875.

(19) Luo, W.; Xu, X.; Luo, S.; Nie, Z.; Hiralal, P.; Wang, Y.; Zhou, H. In *The influence of fullerene-based interlayers on CH3NH3PbI3 Perovskite Photodetector*, 2017 IEEE 12th International Conference on Nano/Micro Engineered and Molecular Systems (NEMS), 9−12 April, 2017; pp 574−578.

(20) Chin, X. Y.; Cortecchia, D.; Yin, J.; Bruno, A.; Soci, C. Lead iodide perovskite light-emitting field-effect transistor. *Nat. Commun.* **2015**, *6*, No. 7383.

(21) Wang, G.; Li, D.; Cheng, H. C.; Li, Y.; Chen, C. Y.; Yin, A.; Zhao, Z.; Lin, Z.; Wu, H.; He, Q.; Ding, M.; Liu, Y.; Huang, Y.; Duan, X. Wafer-scale growth of large arrays of perovskite microplate crystals for functional electronics and optoelectronics. *Sci. Adv.* **2015**, *1*, No. e1500613.

(22) Liu, F.; Wang, J.; Wang, L.; Cai, X.; Jiang, C.; Wang, G. Enhancement of photodetection based on perovskite/MoS2 hybrid thin film transistor. *J. Semicond.* **2017**, *38*, No. 034002.

(23) Wang, J.; Liu, F.; Wang, G.; Wang, L.; Jiang, C. Novel organic-perovskite hybrid structure forward photo field effect transistor. *Org. Electron.* **2016**, *38*, 158−163.

(24) Tak, Y. J.; Kim, D. J.; Kim, W. G.; Lee, J. H.; Kim, S. J.; Kim, J. H.; Kim, H. J. Boosting Visible Light Absorption of Metal-Oxide-Based Phototransistors via Heterogeneous In-Ga-Zn-O and $CH_3NH_3PbI_3$ Films. *ACS Appl. Mater. Interfaces* **2018**, *10* (15), 12854−12861.

(25) Bao, C.; Yang, J.; Bai, S.; Xu, W.; Yan, Z.; Xu, Q.; Liu, J.; Zhang, W.; Gao, F. High Performance and Stable All-Inorganic Metal Halide Perovskite-Based Photodetectors for Optical Communication Applications. *Adv. Mater.* **2018**, No. e1803422.

(26) Xu, X.; Chueh, C.-C.; Jing, P.; Yang, Z.; Shi, X.; Zhao, T.; Lin, L. Y.; Jen, A. K. Y. High-Performance Near-IR Photodetector Using Low-Bandgap MA0.5FA0.5Pb0.5Sn0.5I3 Perovskite. *Adv. Funct. Mater.* **2017**, *27*, No. 1701053.

(27) Tournebize, A.; Bussière, P.-O.; Rivaton, A.; Gardette, J.-L.; Medlej, H.; Hiorns, R. C.; Dagron-Lartigau, C.; Krebs, F. C.; Norrman, K. New Insights into the Mechanisms of Photodegradation/Stabilization of P3HT:PCBM Active Layers Using Poly(3-hexyl-d13-Thiophene). *Chem. Mater.* **2013**, *25*, 4522−4528.

(28) Kognovitsky, S. O.; Kamanina, N. V.; Seisyan, R. P.; Gaevski, M. E.; Nesterov, S.; Baidakova, M.; Rymalis, M. In *Impact of laser and X-ray irradiation on C 60 films, Nonresonant Laser-Matter Interaction (NLMI-10)*, International Society for Optics and Photonics, 2001; pp 91−97.

(29) Chambon, S.; Rivaton, A.; Gardette, J.-L.; Firon, M. Photo- and thermal degradation of MDMO-PPV:PCBM blends. *Sol. Energy Mater. Sol. Cells* **2007**, *91*, 394−398.

(30) Wei, J.; Li, H.; Zhao, Y.; Zhou, W.; Fu, R.; Leprince-Wang, Y.; Yu, D.; Zhao, Q. Suppressed hysteresis and improved stability in perovskite solar cells with conductive organic network. *Nano Energy* **2016**, *26*, 139−147.

(31) Xu, J.; Buin, A.; Ip, A. H.; Li, W.; Voznyy, O.; Comin, R.; Yuan, M.; Jeon, S.; Ning, Z.; McDowell, J. J.; Kanjanaboos, P.; Sun, J. P.; Lan, X.; Quan, L. N.; Kim, D. H.; Hill, I. G.; Maksymovych, P.; Sargent, E. H. Perovskite-fullerene hybrid materials suppress hysteresis in planar diodes. *Nat. Commun.* **2015**, *6*, No. 7081.

(32) Green, M. A.; Ho-Baillie, A.; Snaith, H. J. The emergence of perovskite solar cells. *Nat. Photonics* **2014**, *8*, 506−514.

(33) Xie, C.; Yan, F. Enhanced performance of perovskite/organic-semiconductor hybrid heterojunction photodetectors with the electron trapping effects. *J. Mater. Chem. C* **2018**, *6*, 1338−1342.

(34) Xie, C.; You, P.; Liu, Z.; Li, L.; Yan, F. Ultrasensitive broadband phototransistors based on perovskite/organic-semiconductor vertical heterojunctions. *Light: Sci. Appl.* **2017**, *6*, No. e17023.
(35) Gong, X.; Tong, M.; Xia, Y.; Cai, W.; Moon, J. S.; Cao, Y.; Yu, G.; Shieh, C. L.; Nilsson, B.; Heeger, A. J. High-detectivity polymer photodetectors with spectral response from 300 nm to 1450 nm. *Science* **2009**, *325*, 1665−1667.
(36) Jeon, S.; Kim, S. I.; Park, S.; Song, I.; Park, J.; Kim, S.; Kim, C. Low-Frequency Noise Performance of a Bilayer InZnO−InGaZnO Thin-Film Transistor for Analog Device Applications. *IEEE Electron Device Lett.* **2010**, *31*, 1128−1130.
(37) Jeong-Min, L.; Woo-Seok, C.; Chi-Sun, H.; In-Tak, C.; Hyuck-In, K.; Jong-Ho, L. Low-Frequency Noise in Amorphous Indium−Gallium−Zinc-Oxide Thin-Film Transistors. *IEEE Electron Device Lett.* **2009**, *30*, 505−507.